# Dispersion interpretation from synthetic seismograms and multi-channel analysis of surface waves (MASW)

*J. Tyler Schwenk*, Richard Miller, Julian Ivanov, Kansas Geological Survey, The University of Kansas*
*Steve Sloan, Jason McKenna US Army Corps of Engineers*

**Summary**

Synthetic seismograms and multi-channel analysis of surface waves (MASW) enhance interpretations of a field site's velocity characteristics. MASW layer models were numerically modeled to produce synthetic shot gathers. Iteratively updating the P- and S-wave synthetic velocity models created shot gathers with first-arrivals and Rayleigh-wave dispersion that closely matched field data. The resulting velocity models gave an estimation of the *Vp*:*Vs* ratio. Dispersion images generated from synthetic shot-gather subsets linked acquisition parameters to modal phenomena observed in initial processing of field data. Similar comparisons gave qualitative estimations of phase-velocity averaging over the spread-length for specific frequency bands. We suggest integrating modeling, using MASW *Vs* interval velocities, to differentiate between true velocity structure and transformation artifacts.

**Introduction**

Rayleigh wave dispersion is used to estimate the S-wave structure of the subsurface. Engineering and environmental applications use the ability of surface waves to map rigidity as a function of lateral and vertical heterogeneities in shear-wave velocity (Socco et al., 2010). By their physical nature, Rayleigh waves propagate as the interference of P- and S-waves along the free surface. Investigation depth is a function of frequency and attenuation. Moreover, since velocity varies with depth, dispersion results as various frequencies travel within different velocity horizons of the subsurface. The phase velocities of individual layers result in surface-wave dispersion as seen on shot gathers. We use multi-channel analysis of surface waves (MASW) for S-wave velocity estimations (Miller et al., 1999).

Surface-wave investigations have included: depth to bedrock (Miller et al., 1999), comparison with refraction microtremor analysis (Anderson et al., 2007; Richwalski et al., 2007; Stephenson et al., 2005), hydrophone acquisition (Kaufmann et al., 2005), pavement characterization (Ryden et al., 2004), and time-lapse study of levees (Ivanov et al., 2005; Ivanov et al., 2006). Others have studied the incorporation of higher-modes within inversion (Luo et al., 2007; Maraschini et al., 2010; Xia et al., 2003) and dispersion imaging (Dal Moro et al., 2003; Duputel et al., 2010; Luo et al., 2008).

There are three parts in the MASW method: acquisition, dispersion-curve processing, and inversion. Acquisition techniques include both passive and active approaches. Passive often generates lower-frequency energy that may be complimentary to active data (Louie, 2001; Park et al., 2007; Strobbia and Cassiani, 2011). A standard approach to active data uses off-end shooting to create common-source gathers. The use of low-frequency (<10 Hz) geophones improves broadband sampling of Rayleigh-wave dispersion (Ivanov et al., 2008). Field records are transformed to the phase-velocity vs. frequency domain using the phase shift method (Park et al., 1998). Dispersion overtone images, as a function of phase-velocity and frequency, are interpreted for the modal curve(s). Some methods solve for an 'effective or apparent' curve (Gucunski and Woods, 1992) which eliminates the need to designate distinct modes (Rix and Lai, 1998; Socco et al., 2002). Depending upon the survey technique optimizing the source-offset and spread-length window for dispersion-curve clarity may be an iterative process (Ivanov et al., 2008; Socco et al., 2009). These curvilinear events are then inverted to form a series of 1D S-wave velocity profiles assigned to the original x-t domain midpoint (Xia et al., 1999). Sequential 1D velocity profiles are then joined into a pseudo-2D profile through interpolation.

Sensitivity testing has included method resolution (Boiero and Socco, 2010; O'Neill et al., 2008; Xia et al., 2005; Xia et al., 2007) and repeatability (Cornou et al., 2006; Beaty and Schmitt, 2003). Complicated *Vs* structures introduce significant subjectivity in dispersion interpretations. Velocity inversions and/or high stiffness contrasts create an increased risk of invalid dispersion characterization and resulting inverted *Vs* profiles. Conversely, such complications may be adequately constrained with *a priori* knowledge. Well-posed inversion problems have proven reliable and repeatable for a wide range of simplistic and complicated *Vs* geometries.

Conventional MASW assumes forward-propagating plane surface waves dominate the shot gather. The inclusion and mixing of coherent noise is generally ignored due to the lower attenuation and higher relative amplitudes of ground roll. The optimum offset distance for proper formation and processing of Rayleigh waves is often determined during acquisition. Rules of thumb have been developed, but are routinely disputed with actual field application (Xia et al., 2009; Xu et al., 2006; Zhang et al., 2004).

Imperfect spread parameters may produce images with poor resolution of modes (Foti et al., 2002), higher-mode domination (Cercato et al., 2010; Cornou et al., 2006), near-field non-plane-wave interference (Park et al., 1999), or poor


DOI http://dx.doi.org/10.1190/segam2012-1534.1

sampling of longer wavelengths (Ivanov et al., 2008). Higher-mode dominance is often attributed to high stiffness contrasts and inversely dispersive media (Forbriger, 2003; O'Neill and Matsuoka, 2005; Socco et al., 2002; Tokimatsu et al., 1992). The employment of an apparent dispersion curve, which incorporates superposition of modes, is still vulnerable to inadequate dispersion imaging. Apparent-curve inversion is insufficiently constrained, as opposed to global-search methods, using the more efficient iterative least-squares method. Inversion schemes ultimately rely on 'perfect' imaging of dispersion characteristics. Without rigorous testing, or *a priori* knowledge, a balance between imaging lateral heterogeneity with shorter spreads and adequately sampling longer wavelengths with relatively longer spreads is not intuitive.

We used the algorithm discussed by Zeng et al. (2011) to create synthetic seismograms that closely match both P-wave first-arrivals and Rayleigh-wave dispersion characteristics of a site located near Yuma, Arizona. The resulting synthetic S- and P-wave velocity models permitted an inference of the site's *Vp*/*Vs* ratio. Spread-length comparison lead to qualitative estimations of lateral heterogeneity and the effects of acquisition parameters on specific frequency segments of dispersion images. Here we suggest the use of modeling to constrain and improve interpretation of Rayleigh-wave dispersion in the presence of complex velocity structures at future sites.

**Method**

Schwenk et al. (2012) used MASW and $S_H$-wave refraction traveltime tomography to constrain each method's starting layer-model at our site near Yuma, Arizona. By using the refraction *Vs* tomogram as *a priori* constraint, along with density and bedrock depth values from well logs, more layers could be included in an updated layer model for inversion. Such treatment allowed for a higher-resolution MASW *Vs* profile while limiting resolution and over-parameterization uncertainties for the MASW section. These findings formulated a characteristic MASW *Vs* model for the site, which formed the basis of synthetic seismic modeling.

Continuing this research, numerical modeling sought to increase the confidence in the dispersion interpretations for the site. The modeling algorithm took density, *Vp*, and *Vs* model inputs to generate synthetic shot gathers. The resulting synthetic P-wave first arrivals were compared to several field gathers and resulted in a RMS error of approximately 9ms. Corresponding iterative updates of the *Vs* models lead to a convergence of the synthetic and field phase-velocity curves of the fundamental and first-higher modes. The *Vp*:*Vs* ratio of the synthetic velocity models was 1.7, reaffirming previous values from independent *Vp/Vs* tomography and MASW surveys.

**Results**

Below is a 2D plot of the 11-layer half-space model used to generate the synthetic seismogram. The source wavelet was a 35Hz center-frequency first-order Gaussian derivative. Simulating the field layout, the source offset was 1.2m from the first geophone with a 1.2m geophone spacing. The common-source gather consisted of 147 geophones. The full-spread seismogram, generated using the above parameters, was used for further processing; a characteristic field gather is also presented (Figure 1).

Full spread images closely match theoretical curves calculated by Schwab and Knopoff (1972). Reductions in spread length resulted in a separation of apparent phase-velocity at 10 Hz for both field and synthetic data sets (Figure 2). This separation is not a function of lateral heterogeneity. Analysis of modeled dispersion images confirms that direct higher-mode interference and superposition is negligible. The velocity pull-down is attributed to spectral leakage and smearing within the frequency domain, resulting in a loss of resolution.

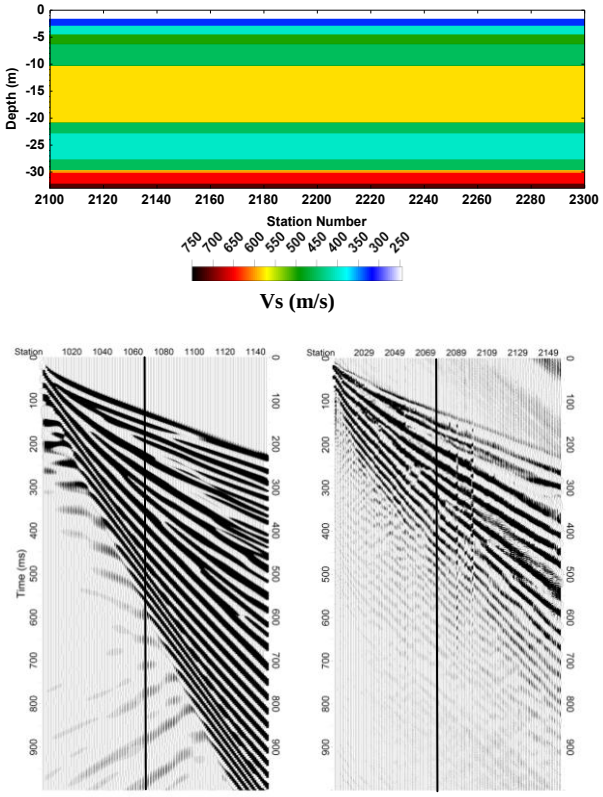


**Figure1:** (Upper) Characteristic velocity model for the YPG site. (Lower) Corresponding synthetic seismogram at right and field shot gather at left with identical acquisition geometries. The optimized 65-geophone spread is left of the vertical lines.



DOI http://dx.doi.org/10.1190/segam2012-1534.1

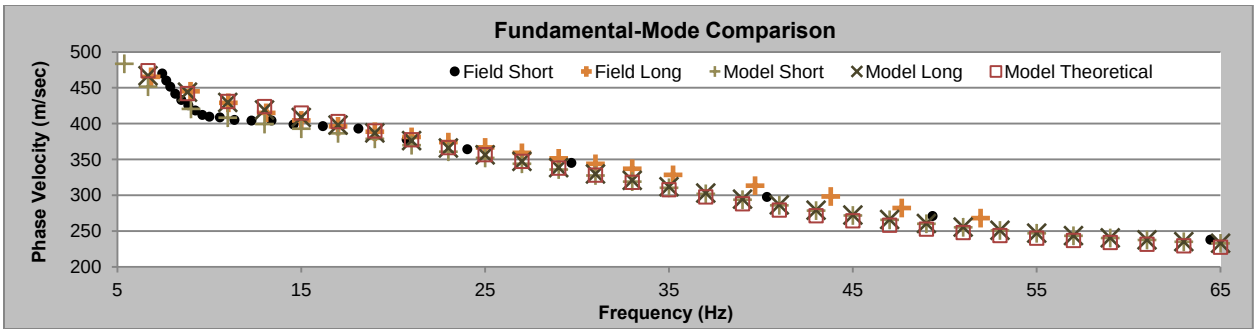


**Figure 2:** Graph of phase-velocity variation with spread length. All subsets have a 1 m source offset, where short refers to a 78m 65-geophone spread and long refers to a 178m 147-geophone spread. At maximum deviation, percent difference is under 6% for corresponding spread lengths. The slight overestimation at high-frequencies is a result of the automatic picking routine.

The slight separation above 25 Hz, observed in field data, is inferred as spread-length averaging induced by lateral heterogeneity. These frequency-dependent effects of the domain transformation were associated with an optimized spread length. The 65-geophone gather was obtained from a systematic sampling of field data resulting in an optimal spread-length and source-offset subset which balanced image and lateral-velocity resolution.

Longer source-offsets resulted in mode superposition and higher-mode velocity pull-ups of the fundamental in the same frequency-band that was affected by spectral leakage (Figure 3). Field data suffered more than modeled data from these effects; this is believed to be due to attenuation effects and additive coherent signal from local heterogeneity not incorporated into the synthetic *Vs* model. The combined effect produced a zigzag phase-velocity trend that was the most compelling evidence for using closer source-offsets within the optimized spread-length.

Modeling increased confidence in modal designation and final *Vs* sections by confirming a small difference between the calculated theoretical curves and fundamental-mode interpretation. This research reiterates that a coupling of closer offsets and long spread-lengths may be necessary to properly image some inversely dispersive *Vs* structures (Ivanov et al., 2011). Although using close offsets is counter-intuitive to sampling longer wavelengths, when considering the model data, the short-offset optimized spread resulted in a 6% maximum underestimation of *Vs* and a preservation of the modal sinuosity with enhanced lateral resolution.

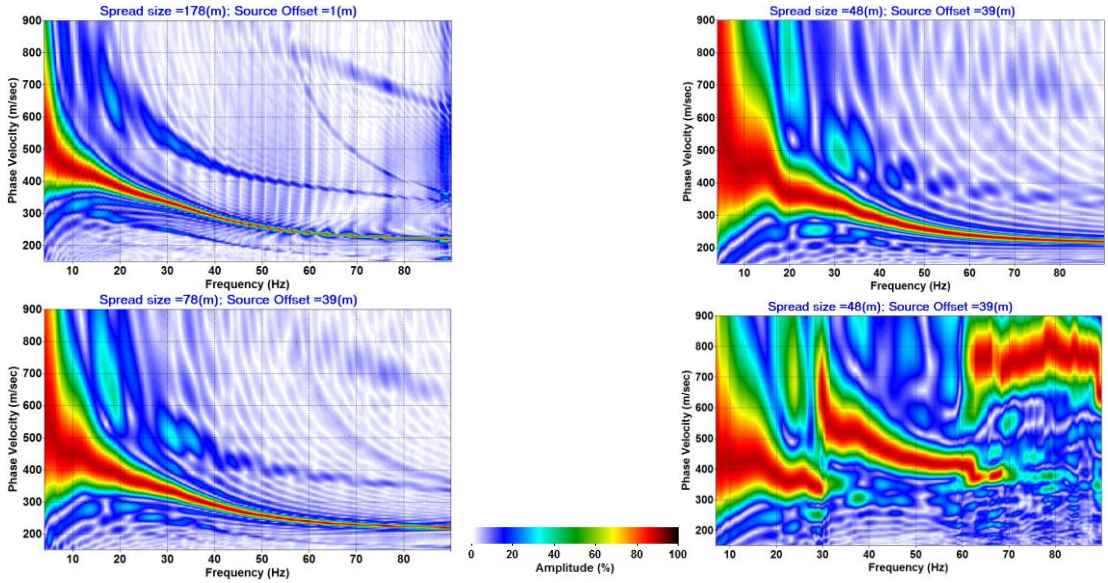


**Figure 3:** Three acquisition subsets are illustrated; all are synthetic except the bottom-right image which is field data. Note the velocity misinterpretation around 10 Hz and increased higher-mode energy. Vertical normalization highlights the curves' maximum-amplitude center.





DOI http://dx.doi.org/10.1190/segam2012-1534.1

The field data was affected by attenuation, resulting in incoherent and discontinuous fundamental-mode signatures below a 200-800 ms sloping 'timeline'. Conversely, the elastic-modeling algorithm didn't incorporate attenuation analysis into wave propagation. This discrepancy between the synthetic and field data was approximated with muting (Ivanov et al., 2005). A long-taper bottom mute was applied to both data along this slope to introduce attenuation. The field data showed little change in the dispersion image, while the modeled image saw a drop in the high-frequency amplitudes of the fundamental (Figure 4). Muting on synthetic gathers enhanced the cut-off frequency around 30 Hz past which the fundamental-mode became over-estimated and the true trend was obscured in field data. This suggests that attenuation and near-field near-surface scattering of the fundamental-mode Rayleigh wave may intensify the affects of higher-mode excitement and hamper dispersion interpretation after domain transformation.

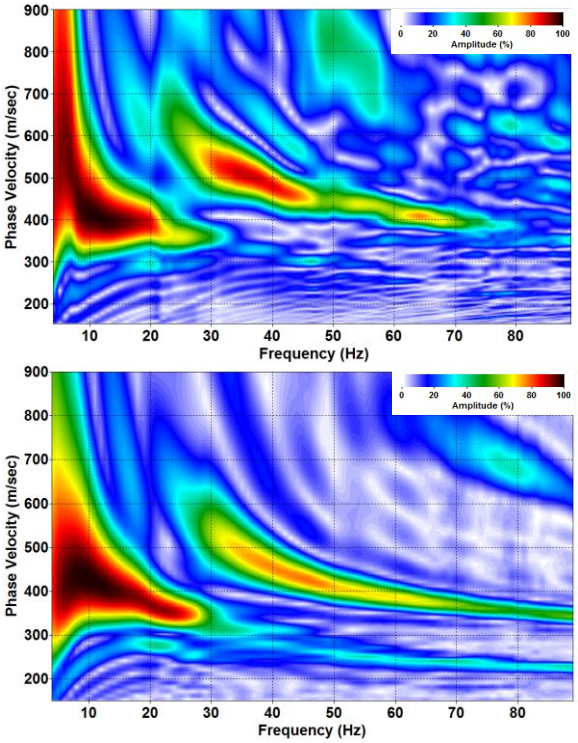


**Figure 4:** (Upper) Field data with bottom mute from 125 ms to 375 ms with a 78m spread and 1.2 m source offset; (Lower) same mute and acquisition parameters applied to the synthetic record. The field data showed little change with muting as signal energy was already attenuated.

## Conclusion

Complicated *Vs* structures introduce some speculation when interpreting dispersion images. Selecting optimal acquisition parameters may be seriously under-constrained without ample site analysis. For our inversely dispersive model, analysis of the processed waveform was negatively affected by loss of resolution and the finite windowing of the x-t domain; which agrees with previous research. Comparison of low-frequency synthetic data with complimentary field gathers verified that the modal responses of certain data were an effect of wavelength sampling and domain transformation rather than local heterogeneity, as appeared to be the case independently. Understanding how modal curves were affected by spatial sampling and acquisition parameters increased confidence in the optimal spread length and dispersion interpretations used in preliminary MASW investigations.

Classical research suggests a proper source offset is equal to the maximum depth of investigation (half the longest wavelength); in this case, approximately 40m. This rule of thumb caused erroneous modal trends and a 10% maximum overestimation of phase velocity. Non-optimal spreads were shown to add or increase the severity of modal inflection points, which could introduce inversion instability. On the other hand, a short offset resulted in a more sinuous curve that underestimated velocities by approximately 6%. These outcomes suggest that shorter offsets, together with longer spread lengths, may be preferable to improve sampling of long wavelengths.

If dispersion interpretation would ignore zig-zag patterns and introduce some smoothing constraint on modal sinuosity, one might minimize the effects of imperfect acquisition parameter sets. For new sites, however, past experience and best-guess interpretation is often what geoscientists must rely on for preliminary interpretations. Data-driven methodologies are always preferable and adding synthetic modeling to compliment MASW investigations may give greater insight into modal trends and their interpretation for future surveys.

## Acknowledgments

Much appreciation goes to Chong Zeng for his development of the modeling software and discussion of its implementation. We would also like to thank Shelby Peterie, Brett Bennett, Benjamin Rickards, Joseph Kearns, Owen Metheny, Anthony Wedel, Brett Wedel, and Joe Anderson for their help in acquiring the field data.



DOI http://dx.doi.org/10.1190/segam2012-1534.1

http://dx.doi.org/10.1190/segam2012-1534.1

**EDITED REFERENCES**

Note: This reference list is a copy-edited version of the reference list submitted by the author. Reference lists for the 2012 SEG Technical Program Expanded Abstracts have been copy edited so that references provided with the online metadata for each paper will achieve a high degree of linking to cited sources that appear on the Web.

**REFERENCES**

Anderson, N., T. Thitimakorn, A. Ismail, and D. Hoffman, 2007, A comparison of four geophysical methods for determining the shear wave velocity of soils: Environmental and Engineering Geoscience, **13**, no. 1, 11–23.

Beaty, K. S., and D. R. Schmitt, 2003, Repeatability of multimode Rayleigh-wave dispersion studies: Geophysics, **68**, 782–790.

Billington, E. D., R. J. Palm, and A. T. Grosser, 2006, MASW imaging of an abandoned Minnesota mine: Proceedings of the Symposium on the Application of Geophysics to Engineering and Environmental Problems (SAGEEP), 482–491.

Boiero, D., and L. V. Socco, 2010, Retrieving lateral variations from surface wave dispersion curves: Geophysical Prospecting, **58**, 997–996.

Casto, D. W., B. Luke, C. Calderon-Macias, and R. Kaufmann, 2009, Interpreting surface-wave data for a site with shallow bedrock: Journal of Environmental and Engineering Geophysics, **14**, 115–127.

Cercato, M., F. Cara, E. Cardarelli, G. DiFilippo, G. DiGuilio, and G. Milana, 2010, Surface-wave velocity profiling at sites with high stiffness contrast: A comparison between invasive and noninvasive methods: Near Surface Geophysics, **8**, 75–94.

Cornou, C., M. Ohrnberger, D. M. Boore, K. Kudo, and P.-Y. Bard, 2006, Derivation of structural models from ambient vibration array recordings: Results from an international blind test: Proceedings of the 3rd International Symposium on the Effects of Surface Geology on Seismic Motion, paper NBT.

Dal Moro, G., E. F. Pipan, and P. Gabrielli, 2003, Determination of Rayleigh wave dispersion curves for near surface applications in unconsolidated sediments: 73rd Annual International Meeting, SEG, Expanded Abstracts, 1049–1052.

Duputel, Z., M. Cara, L. Rivera, and G. Herquel, 2010, Improving the analysis and inversion of multimode Rayleigh-wave dispersion by using group-delay time information observed on arrays of high-frequency sensors: Geophysics, **75**, no. 2, R13–R20.

Forbriger, T., 2003, Inversion of shallow-seismic wavefields: I. Wavefield transformation: Geophysical Journal International, **153**, 719–734.

Foti, S., L. Sambuelli, L. V. Socco, and C. Strobbia, 2002, Spatial sampling issues in *f-k* analysis of surface waves: Proceedings of the Symposium on the Application of Geophysics to Engineering and Environmental Problems (SAGEEP), 12SEI8.

Gucunski, N., and R. D. Woods, 1991, Use of Rayleigh modes in interpretation of SASW test: Proceedings of the 2nd International Conference on Recent Advances in Geotechnical Earthquake Engineering and Soil Dynamics, 1399–1408.

Ivanov, J., R. D. Miller, J. B. Dunbar, and S. Smullen, 2005a, Time-lapse seismic study of levees in southern Texas: 75th Annual International Meeting, SEG, Expanded Abstracts, 1121–1124.

Ivanov, J., R. D. Miller, S. Peterie, C. Zeng, J. Xia, and T. Schwenk, 2011, Multi-channel analysis of surface waves (MASW) of models with high shear-wave velocity contrast: 81st Annual International Meeting, SEG, Expanded Abstracts, 1384–1390.

Ivanov, J., R. D. Miller, N. Stimac, R. F. Ballard, J. B. Dunbar, and S. Smullen, 2006, Time-lapse seismic study of levees in southern Texas: 76th Annual International Meeting, SEG, Expanded Abstracts, 3255–3258.

Ivanov, J., R. D. Miller, and G. Tsoflias, 2008, Some practical aspects of MASW analysis and processing: Proceedings of the Symposium on the Application of Geophysics to Engineering and Environmental Problems (SAGEEP), 1186–1198.

Ivanov, J., C. B. Park, R. D. Miller, and J. Xia, 2005a, Analyzing and filtering surface-wave energy by muting shot gathers: Journal of Environmental and Engineering Geophysics, **10**, 307–322.

Ivanov, J., G. Tsoflias, R. D. Miller, and J. Xia, 2009, Practical aspects of MASW inversion using varying density: Proceedings of the Symposium on the Application of Geophysics to Engineering and Environmental Problems (SAGEEP), 171–177.

Kaufmann, R. D., J. Xia, R. C. Benson, L. B. Yuhr, D. W. Casto, and C. B. Park, 2005, Evaluation of MASW data acquired with a hydrophone streamer in a shallow marine environment: Journal of Environmental and Engineering Geophysics, **16**, no. 2, 87–98.

Lai, C. G., and G. J. Rix, 1998, Simultaneous inversion of Rayleigh phase velocity and attenuation for near-surface site characterization: Georgia Institute of Technology, School of Civil and Environmental Engineering Report GIT-CEE/GEO-98-2.

Louie, J. N., 2001, Faster, better: Shear-wave velocity to 100 meters depth from refraction microtremor arrays: Bulletin of the Seismological Society of America, **91**, no. 2, 347–364.

Luo, Y., J. Xia, Q. Liu, and S. Xu, 2007, Joint inversion of high-frequency surface waves with fundamental and higher modes: Journal of Applied Geophysics, **62**, 375–384.

Luo, Y., J. Xia, R. D. Miller, Y. Xu, J. Liu, and Q. Liu, 2008, Rayleigh-wave dispersive energy imaging using a high-resolution linear Radon transform: Pure and Applied Geophysics, **165**, 903–922.

Maraschini, M., F. Ernst, S. Foti, and L. V. Socco, 2010, A new misfit function for multimodal inversion of surface waves: Geophysics, **75**, no. 4, G31–G43.

Miller, R. D., J. Xia, C. B. Park, and J. M. Ivanov, 1999, Multichannel analysis of surfaces waves to map bedrock: The Leading Edge, **18**, 1392–1396.

O'Neill, A., T. Campbell, and T. Matsuoka, 2008, Lateral resolution and lithological interpretation of surface-wave profiling: The Leading Edge, **27**, 1550–1563.

O'Neill, A., and Matsuoka, T., 2005, Dominant higher surface-wave modes and possible inversion pitfalls: Journal of Environmental and Engineering Geophysics, **10**, no. 2, 185–201.

Park, C. B., R. D. Miller, and J. Xia, 1998, Imaging dispersion curves of surface waves on multi-channel record: 68th Annual International Meeting, SEG, Expanded Abstracts, 1377–1380.

Park, C., R. Miller, and J. Xia, 1999, Multi-channel analysis of surface waves: Geophysics, **64**, 800–808.

Park, C. B., R. D. Miller, J. Xia, and J. Ivanov, 2007, Multichannel analysis of surface waves (MASW) — Active and passive methods: The Leading Edge, **26**, 60–64.

Richwalski, S., M. Picozzi, S. Parolai, C. Milkereit, F. Baliva, D. Albarello, K. Row-Chowdhury, H. van der Meer, and J. Zschau, 2007, Rayleigh wave dispersion curves from seismological and engineering-geotechnical methods: A comparison at the Bornheim test site (Germany): Journal of Geophysics and Engineering, **4**, 349–361.

Ryden, N., C. B. Park, P. Ulriksen, and R. D. Miller, 2004, Multimodal approach to seismic pavement testing: Journal of Geotechnical and Geoenvironmental Engineering, **130**, 636–645.

Schwab, F. A., and L. Knopoff, 1972, Fast surface wave and free mode computations, *in* B. A. Bolt, ed., Methods in computational physics: Academic Press, 87–180.

Schwenk, J. T., R. Miller, J. Ivanov, S. D. Sloan, and J. R. McKenna, 2012, Joint shear-wave analysis using MASW and refraction traveltime tomography: Proceedings of the Symposium on the Application of Geophysics to Engineering and Environmental Problems (SAGEEP), Compact Disc.

Socco, L. V., D. Boiero, S. Foti, and R. Wisén, 2009, Laterally constrained inversion of ground roll from seismic reflection records: Geophysics, **74**, no. 6, G35–G45.

Socco, L. V., S. Foti, and D. Boiero, 2010, Surface-wave analysis for building near-surface velocity models — Established approaches and new perspectives: Geophysics, **75**, no. 5, 75A83–75A102.

Socco, L. V., C. Strobbia, and S. Foti, 2002, Multimodal interpretation of surface wave data: Proceedings of the 8th Meeting of the Environmental and Engineering Geophysics Society European Section (EEGS-ES), 21–25.

Song, Y. Y., J. P. Castagna, R. A. Black, and R. W. Knapp, 1989, Sensitivity of near-surface shear-wave velocity determination from Rayleigh and Love waves: 59th Annual International Meeting, SEG, Expanded Abstracts, 509–512.

Stephenson, W. J., J. N. Louie, S. Pullammanappallil, R. A. Williams, and J. K. Odum, 2005, Blind shear-wave velocity comparison of ReMi and MASW results with boreholes to 200 m in Santa Clara Valley: Implications for earthquake ground-motion assessment: Bulletin of the Seismological Society of America, **95**, 2506–2516.

Strobbia, C., and G. Cassiani, 2011, Refraction microtremors: Data analysis and diagnostics of key hypotheses: Geophysics, **76**, no. 3, MA11–MA20.

Tokimatsu, K., S. Tamura, and H. Kojima, 1992, Effects of multiple modes on Rayleigh wave dispersion: Journal of Geotechnical Engineering, **118**, 1529–1543.

Xia, J., C. Chen, G. Tian, R. D. Miller, and J. Ivanov, 2005, Resolution of high-frequency Rayleigh-wave data: Journal of Environmental and Engineering Geophysics, **10**, 99–110.

Xia, J., R. D. Miller, and J. Ivanov, 2007, Sensitivity of high-frequency Rayleigh-wave data revisited: 77th Annual International Meeting, SEG, Expanded Abstracts, 1142–1146.

Xia, J., R. D. Miller, and C. B. Park, 1999, Estimation of near-surface velocity by inversion of Rayleigh waves: Geophysics, **64**, 691–700.

Xia, J., R. D. Miller, C. B. Park, and G. Tian, 2003, Inversion of high frequency surface waves with fundamental and higher modes: Journal of Applied Geophysics, **52**, 45–57.

Xia, J., R. D. Miller, X. Yixian, L. Yinhe, C. Chao, L. Jiangping, J. Ivanov, and C. Zeng, 2009, High-frequency Rayleigh-wave method: Journal of Earth Science, **20**, 563–579.

Xu, Y., J. Xia, and R. D. Miller, 2006, Quantitative estimation of minimum offset for multichannel surface-wave survey with actively exciting source: Journal of Applied Geophysics, **59**, 117–125.

Zeng, C., J. Xia, R. D. Miller, and G. P. Tsoflias, 2011, Application of the multiaxial perfectly matched layer (M-PML) to near-surface seismic modeling with Rayleigh waves: Geophysics, **76**, no. 3, T43–T52.

Zhang, S. X., L. S. Chan, and J. Xia, 2004, The selection of field acquisition parameters for dispersion images from multichannel surface wave data: Pure and Applied Geophysics, **161**, 1–17.